UPDATING ABOVEGROUND BIOMASS AT A PAN-EUROPEAN SCALE THROUGH SATELLITE DATA AND ARTIFICIAL INTELLIGENCE

F. Pirotti [1,2*], J.R. González-Olabarria [3,4] E. Kutchartt [1]

[1] Department of Land Environment Agriculture and Forestry (TESAF), University of Padova, Legnaro (PD), Italy – (francesco.pirotti,erico.kutchartt)@unipd.it
[2] Interdepartmental Research Center of Geomatics (CIRGEO), University of Padova, Legnaro (PD), Italy
[3] Forest Science and Technology Centre of Catalonia (CTFC). Solsona, Spain – jr.gonzalez@ctfc.cat
[4] Joint Research Unit CTFC – AGROTECNIO. Solsona, Spain

Commission III, WG III/8

KEY WORDS: stacked ensemble machine learning; global biomass maps; remote sensing; radar; bioclimatic variables

ABSTRACT:

In this work, an ensemble of machine learning algorithms was trained using stratified sampling from an existing European-scale biomass map from 2018 to predict an updated version for 2020. The objective of stratification is to make sure that the full range of biomass values is represented. The sampled biomass values from 2018 were filtered to remove areas that did were subject to forest disturbances between 2018 and 2020. This information was available from forest cover/loss/gain maps derived from satellite imagery. We train using a total of 49 features derived from the following sources: bioclimatic data, maps of land-cover, tree cover, tree height, annual composites of vegetation indices per pixel (EVI and NDVI) obtained from Sentinel-2, radar backscatter median annual values from Sentinel-1 and ALOS-2, and the ALOS DSM (3D) elevation grid. A model was created dividing Europe into 19 tiles to limit variability due to very different bioclimatic zones. The result is a raster with 100 m x 100 m resolution and an estimated value of biomass (Mg ha^{-1}) at each node. Overall results on validation data over Europe report a root mean square error (RMSE) of 32.4 Mg ha^{-1} and a mean absolute error (MAE) of 21.5 Mg ha^{-1}; when considering single tiles, the largest RMSE was 54.7 Mg ha^{-1} in tile D2, which can be explained by the very high variance of climate, environment, terrain topography and biomass values as the tile enclosed the Alpine region and the western part of Eastern Europe.

1. INTRODUCTION

The European Union (EU) is covered by forests for 38% of its total land area. It is important to harmonize the estimates of forest biomass over all of Europe to support EU policies on bioeconomy and renewable resources, to design and implement effective and sustainable forest management practices, and to improve actions on climate change mitigation (Avitabile and Camia, 2018). Forest biomass values fluctuate over time due to natural forest dynamics, management practices, or the impacts of disturbances of biotic or abiotic nature. In addition, it is important to accurately estimate forest biomass, which is also related to row material production, which allows storing carbon in wood products (Verkerk et al., 2019). Due to the abovementioned, it is quite relevant to have technological tools from remote sensing that can permanently and systematically quantify and monitor changes in forest biomass at larger scales.

Several biomass maps at a pan-European and global scale have been produced by many authors in the last decade, such as Kindermann et al., (2008), Gallaun et al., (2010), Barredo et al., (2012), Santoro et al., (2022), and Araza et al., (2023), through varied spatial resolutions (100 m – 1 km). The main inputs for producing maps at large scales are mostly through remote sensing data and field measurements. In remote sensing, the most common products used to compute maps at a pan-European and global scale are MODIS, Landsat, Sentinel (combining active and passive sensors), climate, and land cover data, among other remote sensing inputs. Recently, new missions have been launched related to biomass estimation in the last few years (e.g., NISAR, GEDI, and BIOMASS) (Duncanson et al., 2019). On the other hand, the field measurements consist of plots of fixed area, which can vary from 0.01 to almost 1 ha (Nesha et al., 2022), and in some cases, these plots are permanently measured through national forest inventories (NFI). The ground-truth data is a critical input for training, validating, and, thus, producing accurate maps.

Estimating accuracy of maps with cell resolution that is much larger than the typical area of ground plots in forests is difficult due to the unknown representativeness of ground truth data with respect to the larger pixel if falls in. This issue is also related to the harmonization of the biomass plots and data. Different countries use different sampling designs in data collection and biomass compartment definition, and often have different years of data acquisition, different plot shapes and sizes, and plots that are not uniformly distributed (Vidal et al., 2016; Herold et al., 2019). At the European scale, Avitabile and Camia (2018) reported accuracies among six biomass maps in a range between 57 and 61 relative root mean square error (RMSE). Moreover, global biomass maps have been the goal of several investigations and funded projects. Saatchi et al., (2011) reported uncertainty between ±6% and ±53% of total biomass (above- and below-ground) across large areas, with a more limited ±5% at the national scale. In addition, the coarse spatial resolutions of global biomass maps limit their applications for a

* Corresponding author

more detailed analysis in the quantification of carbon stocks and expected fire behaviour.

To the authors' knowledge, at the time of writing this article, the latest and most detailed maps at global scale with rigorous accuracy assessments have been estimated by the Climate Change Initiative Biomass project for 2018. As reported by the project, "the biomass data are derived from a combination of Earth observation data, depending on the year, from the Copernicus Sentinel-1 mission, Envisat's ASAR instrument, and JAXA's Advanced Land Observing Satellite (ALOS-1 and ALOS-2), along with additional information from Earth observation sources". The AGB is provided in Mg ha^{-1} in the raster dataset. Estimates of above-ground biomass uncertainty expressed as the standard deviation in Mg ha^{-1} are also provided (Santoro and Cartus, 2021).

The main objective of this research was to use different layers from earth observation and derived products that describe features that can be used to predict biomass over the Earth's surface. Features considered are related to canopy height, canopy cover, vegetation types, annual composites of NDVI using Sentinel-2 data, SAR backscatter, an elevation grid (ALOS 3D), and bioclimatic variables. These independent data are used to predict aboveground biomass through the artificial intelligence (AI) approach of stacked ensemble machine learning (ML) learners.

2. MATERIALS AND METHODS

We build on the results of the Biomass_CCI to provide an updated version of AGB at European scale with 100 m resolution for the year 2020.

2.1 Features

The variables used as features (independent variables) are the following 49 potential covariates. Data sources came from various raster grids that were resampled at 100 m resolution. Where the original data was at a higher resolution, an appropriate aggregation operator was applied depending on the variable. Where the original data resolution was considerably lower, e.g., bioclimatic features - resolution at 1 km – simple linear interpolation was used. Below, the variables are reported and described.

- 19 bioclimatic variables resolution from the WorldClim database created at University of California, Berkeley – ~1 km resolution (Hijmans et al., 2005);
  - bio01 Annual mean temperature
  - bio02 Mean diurnal range
  - bio03 Isothermality (bio02/bio07)
  - bio04 Temperature seasonality
  - bio05 Max temperature of warmest month
  - bio06 Min temperature of coldest month
  - bio07 Temperature annual range (bio05-bio06)
  - bio08 Mean temperature of wettest quarter
  - bio09 Mean temperature of driest quarter
  - bio10 Mean temperature of warmest quarter
  - bio11 Mean temperature of coldest quarter
  - bio12 Annual precipitation
  - bio13 Precipitation of wettest month
  - bio14 Precipitation of driest month
  - bio15 Precipitation seasonality
  - bio16 Precipitation of wettest quarter
  - bio17 Precipitation of driest quarter
  - bio18 Precipitation of warmest quarter
  - bio19 Precipitation of coldest quarter
- 1 topographic feature, Earth surface elevation (digital surface model – DSM) from ALOS World 3D - ~30m resolution dataset (Tadono et al., 2016, 2014);
- 2 canopy-related features
  - canopy heights - ~10 m resolution aggregated at 100 m with the average heights (Lang et al., 2022)
  - canopy cover fraction – global canopy cover map updated to 2020 using the loss/gain layer map – original resolution ~30 m (Hansen et al., 2013)
- 2 vegetation indices from optical Landsat 8 annual composites of the 95th percentile values – 30 m original resolution, resampled to 100 m using the median operator for spatial aggregation.
  - Enhanced Vegetation Index (EVI) (Main et al., 2011)
  - Normalized Difference Vegetation Index (NDVI)
- 5 land cover maps at 10 m resolution: one map with aggregated overall majority land cover class in the 100 m x 100 m pixel and 4 with fractional information of the different vegetation classes (forest, shrubland, grassland, and agriculture) - (Zanaga et al., 2021);
- 4 RADAR backscatter features,
  - 2 from ALOS, HH, and HV polarization – 25 m resolution, resampled with median values inside the 100 m final resolution (Shimada et al., 2014).
  - 2 features from Sentinel-1, VV and VH polarization of C-Band backscatter available from GEE pre-processed with Sentinel-1 Toolbox for (i) thermal noise removal (ii), and radiometric calibration (iii) terrain correction. The final terrain-corrected values are converted to decibels via log scaling (10*log10(x)). We then processed for correcting for incidence angle (Pirotti et al., 2023) using ALOS 3D, which has an accuracy <10m for height values; Aggregation was done over time and space. Time-wise the Sentinel-1 backscatter from VV and VH polarizations was aggregated with median values over the summer months of the year 2020 (01 June 2020 to 01 September 2020). This was done to minimize the effect, on backscatter RADAR values, of snow and ice in the canopy at higher elevations and at higher latitudes. Space-wise the 10 m pixels were mapped to a 100 m final resolution with median values as well;
- 16 vegetation types map - 1 overall vegetation class of type with the highest probability was derived from these maps (Bonannella et al., 2022). It should be noted that these are small scale probability maps estimated from AI. As such, they represent the probability of a species being present according to bioclimatic and other factors, but do not imply that the vegetation cover is in reality from that species. More detailed maps using high resolution imagery might be provided in the future (Gazzea et al., 2022).

2.2 Training and testing

For training and testing, we grouped the dependent variable values, i.e., the AGB values, in 10 classes each of size 50 Mg ha^{-1} to provide 10 strata that are then used for stratified sampling. The goal of this approach is to give a balanced representation of the total range of biomass values. The AGB values used for training and testing were taken from the 2018 global datasets of forest above-ground biomass of the European Space Agency Biomass Climate Change Initiative (Santoro and Cartus, 2021; Santoro et al., 2022). A total of ~200'000 sampled locations are used for training and the same amount for

testing. The area was divided into 19 tiles, 13 of which covered the European Union and were ultimately used (see figure 1 below). This was done to limit the variance of the different variables used and create specific models in a more constrained area.

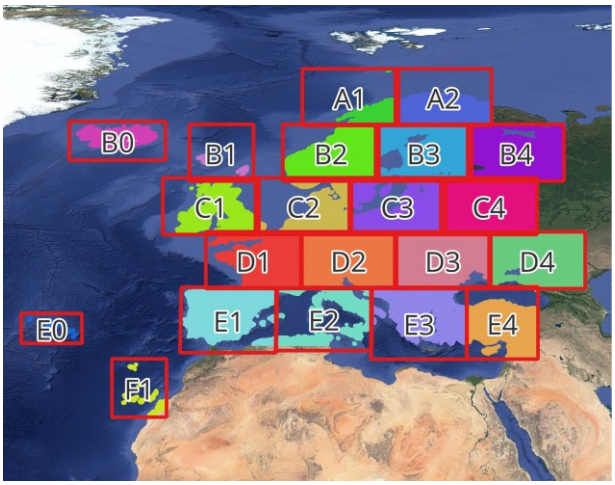

Figure 1. Tiles covering also the European union area for specific model training

The rationale of this method is that, in an ideal situation, training should be done with ground-measured data. But it is very seldom the case that there are a significant number of large forest plots (1 ha) available with biomass values at the year of interest and that they are numerically representative of the extremely varied biomass scenarios in Europe. Therefore, for training, we used biomass data that had been estimated from previous work. These data will have a larger error with respect to ground measures, but the very high number that we can use with this approach allows the machine learning ensemble to minimize the effect of the error. Except for the bioclimate maps and the DSM, all other features are from the year 2020.

2.3 AI Algorithms

Training, testing, and prediction were done using the H2O library implemented in the R-CRAN environment (Candel and LeDell, 2022; LeDell et al., 2022). The choice was driven by the intrinsic capability of the library to leverage multiple CPUs via parallelization and thus provide higher computing capabilities when used on multi-CPU high-performance computing (HPC) systems. In this study, a 16 CPU Linux machine with 256 MB of RAM was used. Version 3.38.0.3 of H2O was used. A total of 13 models were created with training data, one for each tile that overlaps the main European Union area. Models are available upon request in Model ObJect, Optimized (MOJO) format.

The regression was carried out using staked ensembles of models. From H2O documentation, “stacked ensemble method is a supervised ensemble machine learning algorithm that finds the optimal combination of a collection of prediction algorithms using a process called stacking”. Ensembles have proven to represent an asymptotically optimal system for learning (Van Der Laan et al., 2007). This approach has also been used for forest monitoring by Healey et al., (2018) for the creation of the Landscape Change Monitoring System (LCMS) data suite with improved map accuracy across a range of ecosystems and change processes.

3. RESULTS

3.1 Accuracy of regression

The test set of values was used to assess the results of running over the full set of features and removing the 16 features related to vegetation species to see the impact on the result. Figure 2 below shows the root mean square error (RMSE) for each tile for the two combinations.

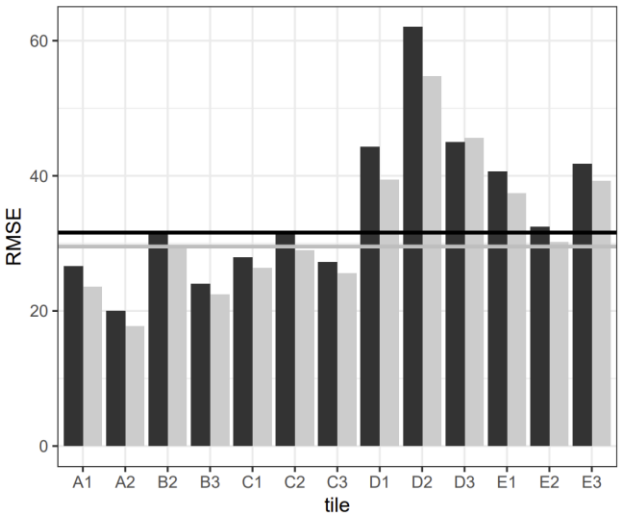

Figure 2. Root mean square error per each tile using 33 features, i.e., all features except vegetation types (black) and all 49 features including vegetation types (grey). RMSE unit is AGB in Mg ha^{-1}

Overall results on validation data over Europe report a root mean square error (RMSE) of 32.4 Mg ha^{-1} and a mean absolute error (MAE) of 21.5 Mg ha^{-1}; when considering single tiles, the largest RMSE was 54.7 Mg ha^{-1} in tile D2 (see Figure 1), which can be explained by the very high variance of biomass values as the tile enclosed the Alpine region and the western part of Eastern Europe.

3.2 Data access and representation

The models trained via the stacked ensemble method were used to predict AGB values across Europe and create an AGB raster and a raster with an estimated standard deviation of the estimated value. Two online web portals were created: (i) one for internal use for analysing the results and also for querying a single location to check the values of all 49 features at that location (Figures 3), and (ii) one for viewing data and downloading rasters of AGB for each country (Figure 4). A further collaborative web-app was developed for collecting ground truth via smartphones for further data validation (Kutchartt et al., in Print), similar to other work that uses collaborative web-tools to collect information (Pirotti et al., 2011, 2022).

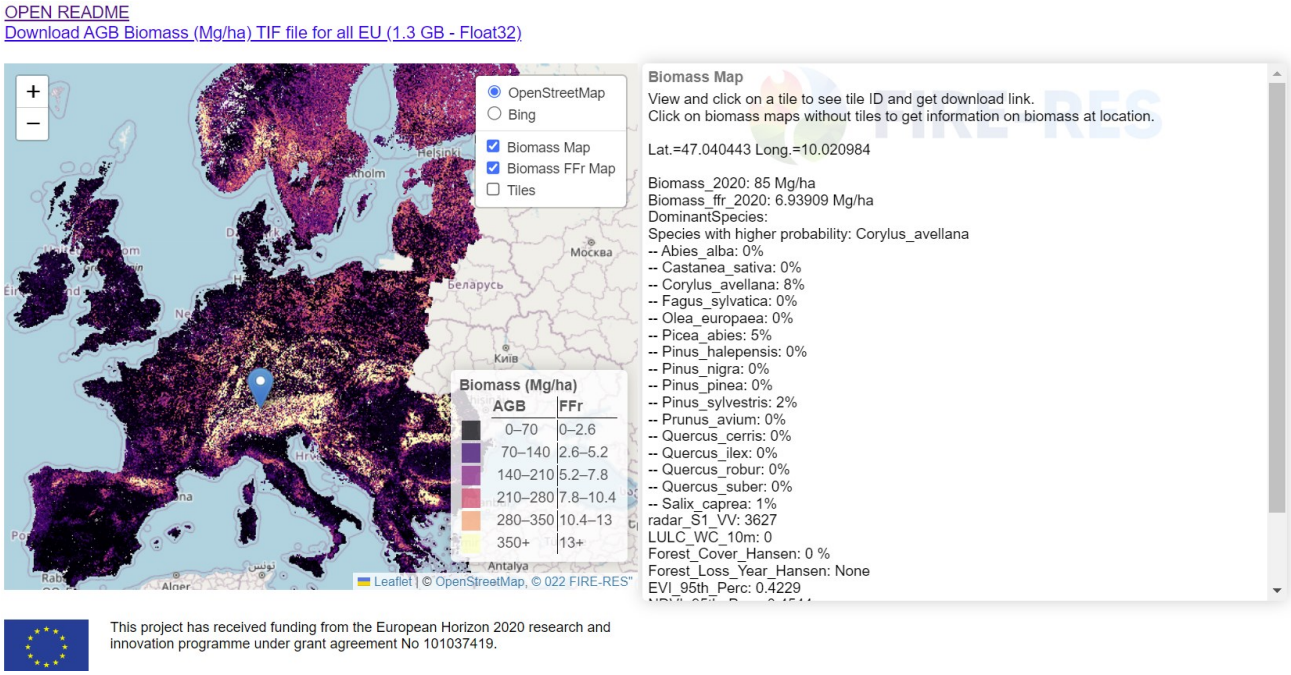

Figure 3. Interactive web-GIS portal for querying biomass values and descriptors at user-defined coordinate.

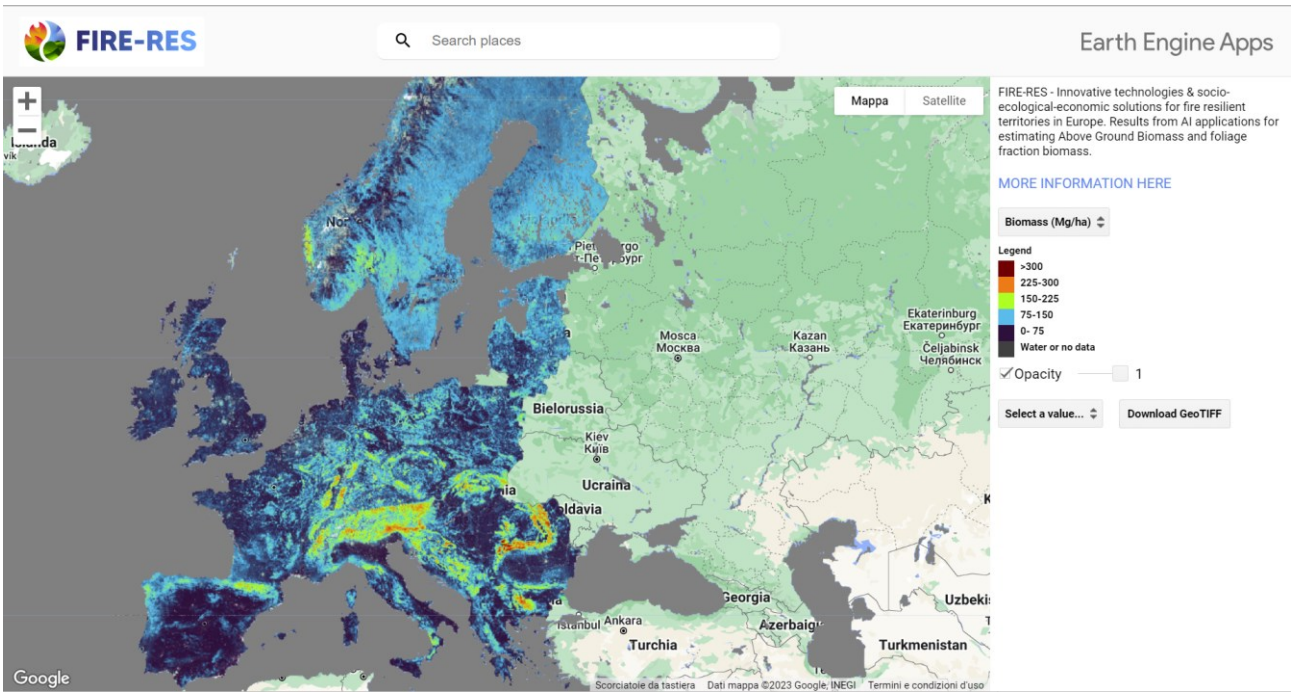

Figure 4. Google Earth Engine App: users can view and download clipped country-specific maps for the total aboveground biomass (Mg ha^{-1}) and their standard deviation (SD) in GeoTIFF format.

Figure 3 shows the internal web portal with location information over the blue marker. This portal connects the data with the user through an interface that allows the user to click a location, and the server returns the values of the features that are available at that specific location. A result of this interaction is seen in Figure 3, where the data extracted at the location of the blue marker is visible on the right side.

Figure 4 shows the other web portal that is available for public access. This was deployed via Google Earth Engine and consists of a viewer and a tool (right side) for downloading AGB maps for each country.

3.3 Comparison with other AGB maps

The Climate Change Initiative Biomass (Biomass_CCI) recently – after the first draft of this paper - produced a map of AGB for the year 2020. Therefore, we analysed the differences between our product and this one. As reported in their documentation, "The primary science objective of ESA's

Climate Change Initiative Biomass project is to provide global maps of above-ground biomass (Mg ha^{-1}) for multiple epochs (2005/07, 2010, 2015/16, and annually for 2017-2022), with these being capable of supporting quantification of biomass change. The mapping will be at 100 m grid spacing with a target relative error of less than 20 % where AGB exceeds 50 Mg ha^{-1}. Although this resolution is finer than required for current climate modelling, it will allow more refined information to be inferred (e.g., forest age structure and the disturbance regime) that is relevant for climate and has the potential to be exploited by carbon cycle and climate models as they develop." The standard deviation of the differences between our map and the ESA Climate Change Initiative map for 2020 is ~55 Mg ha^{-1} with a bias of ~17 Mg ha^{-1}. The bias points toward estimating larger values of biomass in our results with respect to ESA's results. Figure 5 below represents the distribution of differences.

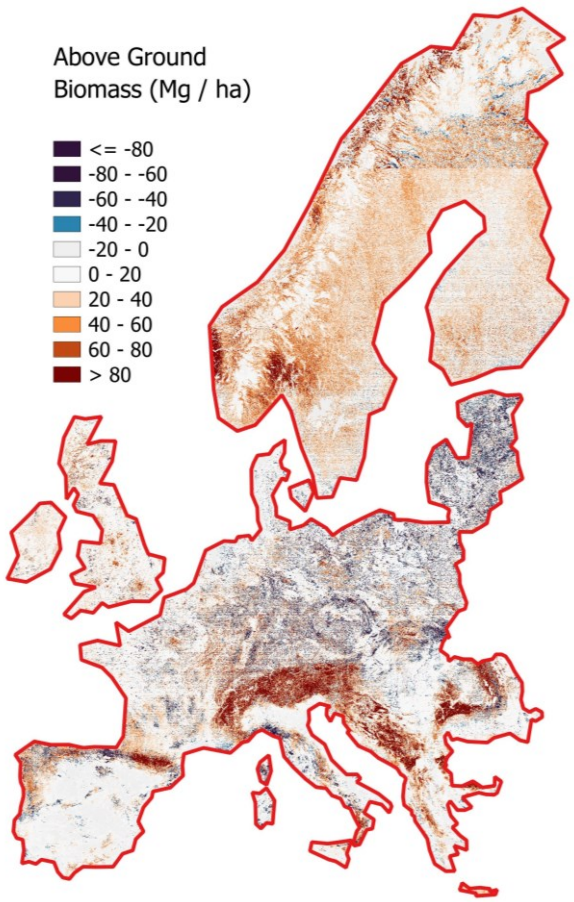

Figure 5. Map of differences between FIRE-RES AGB values and ESA Climate Change Initiative Biomass of 2020.

4. DISCUSSION

There are existing global and regional biomass maps. Authors in Avitabile and Camia (2018) compared four biomass maps between 2008 and 2014 at European scale with pixel resolutions of ⩾~1 km. The coarse spatial resolutions in this case limit their applications to a more detailed analysis of expected fire behaviour. To the authors' knowledge and at the time of writing, the more recent and detailed maps with rigorous accuracy assessment have been estimated by the Climate Change Initiative Biomass (Biomass_CCI) project up to the year 2018, when the project started, with 100 m spatial resolution (Araza et al., 2023). From the same project, updated AGB maps for the year 2020 are now available; therefore, a comparison is possible and was carried out (see Figure 5). It can be noted from the comparison of results that areas in mountain regions have higher biomass values in our results with respect to Biomass_CCI. This should be noted as very likely to be an overestimation by our results due to under-represented samples in that specific scenario.

Mapping vegetation is a key task in many applications, especially considering the more extreme events that are foreseen in the future (Laurin et al., 2021; Piragnolo et al., 2021). The biomass of mapped vegetation is a proxy for the carbon-fixing capabilities of the area and is also one key factor that concurs to estimating fire hazards. Many efforts on mapping biomass have been and are currently ongoing, at different scales and with different methods. Satellite remote sensing is the main source of data for mapping biomass at the regional scale, i.e., the continental scale. The numerous space programs nowadays allow for the acquisition of dense time series of optical and radar imagery that cover all forested land. Converting digital numbers to values of the biomass of its different components, along with an assessment of the expected uncertainty of the results, is challenging.

It should be noted that a rigorous assessment of accuracy would require field samples. There are numerous field samples available from stakeholders and project partners, but they suffer from two main problems: almost all samples have a much smaller size than the 100 m x 100 m area that is the basic unit of our map, and they were sampled at different moments in time. This last problem can be mitigated by applying a general growth model to estimate an updated value of biomass, but this would add further uncertainty to measured values that propagates to the original measurement errors. The first problem might be solved by up-scaling the plot area by a scale factor. This is not an ideal solution, as the variance of the measured value around the plot is unknown. For example, as can be seen in Figure 6 below, a ground sample plot of 10 m radius might "catch" a value of biomass that is not representative of the 100 m x 100 m raster cell, and thus upscaling will provide very wrong values. In Figure 6, the up-scaling would provide an overestimation as the circular plot is over an area with a higher vegetation density than the rest of the area.

Figure 6. 100 m x 100 m area with a hypothetical 10 m radius plot.

5. CONCLUSIONS

In this work, we report preliminary results on using an ensemble of machine learning/artificial intelligence algorithms to provide an updated map at ~100 x 100 m resolution of aboveground biomass. Aboveground biomass is defined as the mass, expressed as oven-dry weight of the woody parts (stem, bark, branches, and twigs) of all living trees, excluding stumps and roots. The mapped aboveground biomass information is to be used for the further definition of fire models across Europe. For this reason, it is important to have the values of AGB as much accurate as possible. Further work will see the extraction of the fraction of biomass from thinner components (branches, foliage), which is a critical variable in fire simulations, as well as the estimation of canopy bulk density and other factors required to support the definition of fuel types.

ACKNOWLEDGEMENTS

This project has received funding from the European Horizon 2020 research and innovation programme under grant agreement No 101037419 - Innovative technologies & socio-ecological-economic solutions for fire resilient territories in Europe - FIRE-RES.

REFERENCES

Araza, A., Herold, M., de Bruin, S., Ciais, P., Gibbs, D.A., Harris, N., Santoro, M., Wigneron, J.-P., Yang, H., Málaga, N., Nesha, K., Rodriguez-Veiga, P., Brovkina, O., Brown, H.C.A., Chanev, M., Dimitrov, Z., Filchev, L., Fridman, J., García, M., Gikov, A., Govaere, L., Dimitrov, P., Moradi, F., Muelbert, A.E., Novotný, J., Pugh, T.A.M., Schelhaas, M.-J., Schepaschenko, D., Stereńczak, K., Hein, L., 2023. Past decade above-ground biomass change comparisons from four multi-temporal global maps. International Journal of Applied Earth Observation and Geoinformation 118, 103274. https://doi.org/10.1016/j.jag.2023.103274

Avitabile, V., Camia, A., 2018. An assessment of forest biomass maps in Europe using harmonized national statistics and inventory plots. Forest Ecology and Management 409, 489–498. https://doi.org/10.1016/j.foreco.2017.11.047

Barredo, J.I., San Miguel, J., Caudullo, G., Busetto, L., 2012. A European map of living forest biomass and carbon stock. Joint Research Centre of the European Commission. 12 p.

Bonannella, C., Hengl, T., Heisig, J., Leal Parente, L., Wright, M., Herold, M., de Bruin, S., 2022. Presence-Absence Points for Tree Species Distribution Modelling for Europe. https://doi.org/10.5281/ZENODO.5818021

Candel, A., LeDell, E., 2022. Deep Learning with H2O.

Duncanson, L., Armston, j., Disney, M., Avitabile, V., Barbier, N., Calders, K., Carter, S., Chave, J., Herold, M., Crowther, T.W., Falkowski, M., Kellner, J.R., Labrière, N., Lucas, R., MacBean, N., McRoberts, R.E., Meyer, V., Næsset, E., Nickeson, J.E., Paul, K.I., Phillips, O.L., Réjou-Méchain, M., Román, M., Roxburgh, S., Saatchi, S., Schepaschenko, D., Scipal, K., Siqueira, P.R., Whitehurst, A., Williams, M., 2019. The importance of consistent global forest aboveground biomass product validation. Surveys in Geophysics 40, 979-999. https://doi.org/10.1007/s10712-019-09538-8

Gazzea, M., Kristensen, L.M., Pirotti, F., Ozguven, E.E., Arghandeh, R., 2022. Tree Species Classification Using High-Resolution Satellite Imagery and Weakly Supervised Learning. IEEE Transactions on Geoscience and Remote Sensing 60, 1–11. https://doi.org/10.1109/TGRS.2022.3210275

Gallaun, H., Zanchi, G., Nabuurs, G.J., Hengeveld, G., Schardt, M., Verkerk, P.J., 2010. EU-wide maps of growing stock and above-ground biomass in forests based on remote sensing and field measurements. Forest Ecology and Management 260, 252-261. https://doi.org/10.1016/j.foreco.2009.10.011

Hansen, M.C., Potapov, P.V., Moore, R., Hancher, M., Turubanova, S.A., Tyukavina, A., Thau, D., Stehman, S.V., Goetz, S.J., Loveland, T.R., Kommareddy, A., Egorov, A., Chini, L., Justice, C.O., Townshend, J.R.G., 2013. High-Resolution Global Maps of 21st-Century Forest Cover Change. Science 342, 850–853. https://doi.org/10.1126/science.1244693

Healey, S.P., Cohen, W.B., Yang, Z., Kenneth Brewer, C., Brooks, E.B., Gorelick, N., Hernandez, A.J., Huang, C., Joseph Hughes, M., Kennedy, R.E., Loveland, T.R., Moisen, G.G., Schroeder, T.A., Stehman, S.V., Vogelmann, J.E., Woodcock, C.E., Yang, L., Zhu, Z., 2018. Mapping forest change using stacked generalization: An ensemble approach. Remote Sensing of Environment 204, 717–728. https://doi.org/10.1016/j.rse.2017.09.029

Herold, M., Carter, S., Avitabile, V., Espejo, A.B., Jonckheere, I., Lucas, R., McRoberts, R.E., Næsset, E., Nightingale, J., Petersen, R., Reiche, J., Romijn, E., Rosenqvist, A., Rozendaal, D.M.A., Seifert, F.M., Sanz, M.J., De Sy, V., 2019. The role and need for space-based forest biomass - related measurements in environmental management and policy. Surveys in Geophysics 40, 757-778. https://doi.org/10.1007/s10712-019-09510-6

Hijmans, R.J., Cameron, S.E., Parra, J.L., Jones, P.G., Jarvis, A., 2005. Very high resolution interpolated climate surfaces for global land areas. International Journal of Climatology 25, 1965–1978. https://doi.org/10.1002/joc.1276

Kindermann, G.E., McCallum, I., Fritz, S., Obersteiner, M., 2008. A global forest growing stock, biomass and carbon map based on FAO statistics. Silva Fennica 42(3), 244. https://doi.org/10.14214/sf.244

Kutchartt, E., González-Olabarria, J.R., Trasobares, A., de-Miguel, S., Cardil, A., Botequim, B., Vassilev, V., Palaiologou, P., Rogai, M., Pirotti, F., in Print. FIRE-RES Geo-Catch: A mobile application to support reliable fuel mapping at a pan-European scale. iForest – Biogeosciences and Forestry.

Lang, N., Jetz, W., Schindler, K., Wegner, J.D., 2022. A high-resolution canopy height model of the Earth. https://doi.org/10.48550/ARXIV.2204.08322

Laurin, G.V., Francini, S., Luti, T., Chirici, G., Pirotti, F., Papale, D., 2021. Satellite open data to monitor forest damage caused by extreme climate-induced events: a case study of the Vaia storm in Northern Italy. Forestry: An International Journal of Forest Research 94(3), 407–416. https://doi.org/10.1093/forestry/cpaa043

LeDell, E., Gill, N., Aiello, S., Fu, A., Candel, A., Click, C., Kraljevic, T., Nykodym, T., Aboyoun, P., Kurka, M., Malohlava, M., 2022. h2o: R Interface for the "H2O" Scalable Machine Learning Platform.

Main, R., Cho, M.A., Mathieu, R., O'Kennedy, M.M., Ramoelo, A., Koch, S., 2011. An investigation into robust spectral indices for leaf chlorophyll estimation. ISPRS Journal of Photogrammetry and Remote Sensing 66(6), 751–761. https://doi.org/10.1016/j.isprsjprs.2011.08.001

Nesha, K., Herold, M., De Sy, V., de Bruin, S., Araza, A., Málaga, N., Gamarra, J.G.P., Hergoualc'h, K., Pekkarinen, A., Ramirez, C., Morales-Hidalgo, D., Tavani, R., 2022. Exploring characteristics of national forest inventories for integration with global space-based forest biomass data. Science of the Total Environment 850, 157788. http://dx.doi.org/10.1016/j.scitotenv.2022.157788

Piragnolo, M., Pirotti, F., Zanrosso, C., Lingua, E., Grigolato, S., 2021. Responding to Large-Scale Forest Damage in an Alpine Environment with Remote Sensing, Machine Learning, and Web-GIS. Remote Sensing 13, 1541. https://doi.org/10.3390/rs13081541

Pirotti, F., Adedipe, O., Leblon, B., 2023. Sentinel-1 Response to Canopy Moisture in Mediterranean Forests before and after Fire Events. Remote Sensing 15, 823. https://doi.org/10.3390/rs15030823

Pirotti, F., Guarnieri, A., Vettore, A., 2011. Collaborative Web-GIS design: a case study for road risk analysis and monitoring. Transactions in GIS 15, 213–226. https://doi.org/10.1111/j.1467-9671.2011.01248.x

Pirotti, F., Piragnolo, M., Guarnieri, A., Boscaro, M., Cavalli, R., 2022. Analysis of Geospatial Behaviour of Visitors of Urban Gardens: Is Positioning via Smartphones a Valid Solution?, in: Borgogno-Mondino, E., Zamperlin, P. (Eds.), Geomatics and Geospatial Technologies, Communications in Computer and Information Science. Springer International Publishing, Cham, pp. 351–365. https://doi.org/10.1007/978-3-030-94426-1_26

Saatchi, S.S., Harris, N.L., Brown, S., Lefsky, M., Mitchard, E.T.A., Salas, W., Zutta, B.R., Buermann, W., Lewis, S.L., Hagen, S., Petrova, S., White, L., Silman, M., Morel, A., 2011. Benchmark map of forest carbon stocks in tropical regions across three continents. Proc. Natl. Acad. Sci. U.S.A. 108, 9899–9904. https://doi.org/10.1073/pnas.1019576108

Santoro, M., Cartus, O., 2021. ESA Biomass Climate Change Initiative (Biomass_cci): Global datasets of forest above-ground biomass for the years 2010, 2017 and 2018, v3. https://doi.org/10.5285/5F331C418E9F4935B8EB1B836F8A91B8

Santoro, M., Cartus, O., Wegmüller, U., Besnard, S., Carvalhais, N., Araza, A., Herold, M., Liang, J., Cavlovic, J., Engdahl, M.E., 2022. Global estimation of above-ground biomass from spaceborne C-band scatterometer observations aided by LiDAR metrics of vegetation structure. Remote Sensing of Environment 279, 113114. https://doi.org/10.1016/j.rse.2022.113114

Shimada, M., Itoh, T., Motooka, T., Watanabe, M., Shiraishi, T., Thapa, R., Lucas, R., 2014. New global forest/non-forest maps from ALOS PALSAR data (2007–2010). Remote Sensing of Environment 155, 13–31. https://doi.org/10.1016/j.rse.2014.04.014

Tadono, T., Ishida, H., Oda, F., Naito, S., Minakawa, K., Iwamoto, H., 2014. Precise Global DEM Generation by ALOS PRISM. ISPRS Ann. Photogramm. Remote Sens. Spatial Inf. Sci. II–4, 71–76. https://doi.org/10.5194/isprsannals-II-4-71-2014

Tadono, T., Nagai, H., Ishida, H., Oda, F., Naito, S., Minakawa, K., Iwamoto, H., 2016. Generation of the 30 M-MESH global digital surface model by ALOS PRISM. Int. Arch. Photogramm. Remote Sens. Spatial Inf. Sci. XLI-B4, 157–162. https://doi.org/10.5194/isprsarchives-XLI-B4-157-2016

Van Der Laan, M.J., Polley, E.C., Hubbard, A.E., 2007. Super Learner. Statistical Applications in Genetics and Molecular Biology 6. https://doi.org/10.2202/1544-6115.1309

Verkerk, P.J., Fitzgerald, J.B., Datta, P., Dees, M., Hengeveld, G.M., Lindner, M., Zudin, S., 2019. Spatial distribution of the potential forest biomass availability in Europe. Forest Ecosystems 6(5), 1-11. https://doi.org/10.1186/s40663-019-0163-5

Vidal, C., Alberdi, I., Redmond, J., Vestman, M., Lanz, A., Schadauer, K., 2016. The role of the European National Forest Inventories for international forestry reporting. Annals of Forest Science 73, 793-806. https://doi.org/10.1007/s13595-016-0545-6

Zanaga, D., Van De Kerchove, R., De Keersmaecker, W., Souverijns, N., Brockmann, C., Quast, R., Wevers, J., Grosu, A., Paccini, A., Vergnaud, S., Cartus, O., Santoro, M., Fritz, S., Georgieva, I., Lesiv, M., Carter, S., Herold, M., Li, L., Tsendbazar, N.-E., Ramoino, F., Arino, O., 2021. ESA WorldCover 10 m 2020 v100. https://doi.org/10.5281/ZENODO.5571936